International Journal of Kinesiology & Sports Science
ISSN: 2202-946X
www.ijkss.aiac.org.au

Head, Neck, Trunk, and Pelvis Tissue Mass Predictions for Older Adults using Anthropometric Measures and Dual-Energy X-Ray Absorptiometry

Charles A.J. Kahelin, Nicole C. George, Danielle L. Gyemi, David M. Andrews*
Department of Kinesiology, University of Windsor 401 Sunset Avenue, Windsor, ON, N9B 3P4, Canada
Corresponding Author: David M. Andrews, E-mail: dandrews@uwindsor.ca

ARTICLE INFO

Article history
Received: May 05, 2020
Accepted: July 27, 2020
Published: July 31, 2020
Volume: 8 Issue: 3

Conflicts of interest: None
Funding: The research was funded by the National Sciences and Engineering Research Council of Canada (NSERC).

ABSTRACT

Background: Regression equations using anthropometric measurements to predict soft (fat mass [FM], lean mass [LM], wobbling mass [WM]) and rigid (bone mineral content [BMC]) tissue masses of the extremities and core body segments have been developed for younger adults (16-35 years), but not older adults (36-65 years). Tissue mass estimates such as these would facilitate biomechanical modeling and analyses of older adults following fall or collision-related impacts that might occur during sport and recreational activities. **Purpose:** The purpose of this study was to expand on the previously established tissue mass prediction equations of the head, neck, trunk, and pelvis for healthy, younger adults by generating a comparable set of equations for an older adult population. **Methods:** A generation sample (38 males, 38 females) was used to create head, neck, trunk, and pelvis tissue mass prediction equations via multiple linear stepwise regression. A validation sample (13 males, 12 females) was used to assess equation accuracy; actual tissue masses were acquired from manually segmented full body Dual-Energy X-ray Absorptiometry scans. **Results:** Adjusted R^2 values for the prediction equations ranged from 0.326 to 0.949, where BMC equations showed the lowest explained variances overall. Mean relative errors between actual and predicted masses ranged from –2.6% to 6.1% for trunk LM and FM, respectively. All actual tissue masses except head BMC ($R^2 = 0.092$) were significantly correlated to those predicted from the equations ($R^2 = 0.403$ to 0.963). **Conclusion:** This research provides a simple and effective method for predicting head, neck, trunk, and pelvis tissue masses in older adults that can be incorporated into biomechanical models for analyzing sport and recreational activities. Future work with this population should aim to improve core segment BMC predictions and develop equations for the extremities.

Key words: Regression Equations, Anthropometry, Core Body Segments, Wobbling Mass, Biomechanical Modeling

INTRODUCTION

The movement of soft tissues (muscle, fat, skin) independent of the underlying bone (i.e., rigid tissue) has been shown to have significant force attenuating effects during highly dynamic human movements, especially those involving impacts (Pain & Challis, 2006; Schmitt & Günther, 2010; Bazrgari et al., 2011) that might be experienced during sport and recreational activities. Consequently, biomechanical models that approximate the human body as a series of rigid-linked segments fail to acknowledge the protective role that soft tissue (i.e., wobbling mass = WM) motion plays in mitigating impact shock in the body, and thus, do not produce justifiable simulations of such rapid movements (Gruber et al., 1998). However, the development and validation of effective biomechanical models that include both rigid and non-rigid (i.e., WM) components is limited by the determination of person- and segment-specific soft (fat mass [FM], lean mass [LM]) and rigid (bone mineral content [BMC]) tissue masses in-vivo.

Regression equations that utilize simple anthropometric measures to accurately predict body segment tissue masses in living people have previously been developed for segments of the lower (Holmes et al., 2005), and upper extremities (Arthurs & Andrews, 2009), as well as the core segments of the body (head, neck, trunk and pelvis) (Gyemi et al., 2017). In these works, the predicted tissue masses were validated against actual tissue masses determined from Dual-Energy X-ray Absorptiometry (DXA) scans using custom regions of interest; a method reported to have good to excellent reliability (Burkhart, Arthurs, & Andrews, 2009). Although the predictive capabilities of these equations for estimating soft and rigid tissue masses were found to be relatively strong in general, the equations are only applicable to, and have only been validated using tissue mass data from healthy, younger adults. In order to facilitate the development of high fidelity, person-specific wobbling mass biomechanical models for analyzing impacts during sport and recreational activities involving other populations (e.g., older, working-age adults),

Published by Australian International Academic Centre PTY.LTD.

http://dx.doi.org/10.7575/aiac.ijkss.v.8n.3p.14

additional equations that account for differences in tissue composition characteristic from all body segments of these populations need to be developed.

Therefore, the purpose of this study was to expand on the previously established tissue mass prediction equations of the head, neck, trunk, and pelvis for healthy, younger adults by generating a comparable set of equations for an older adult population. Consistent with previous work, the equations developed here will be used to determine soft (FM, LM, WM = FM + LM) and rigid (BMC) tissue mass estimates from anthropometric measurements and personal characteristics (sex, age).

METHODS

Participants and Design of Study

One hundred and one healthy, older adults (50 F, 51 M; 36-65 years of age) participated in this regression-based correlational study: mean (SD) age, body mass and height were 49.2 (7.7) years, 78.1 (17.0) kg and 1.70 (0.10) m, respectively. The participants are being referred to as "older adults" because, in comparison to the participants of previous research in this area (16-35 years) (Gyemi et al., 2017), the participants in this study are older. The predictor variables for the regressions were anthropometric measurements of the head, neck, trunk, and pelvis, and person-specific measures of age, sex, height, and body mass. Output variables from the regression analyses were the magnitudes of different tissue masses. The sample size for the regression equation generation sample (see Analyses and Statistics section) was chosen to be above the minimum recommendation for multiple regression analyses of four participants for every one predictor variable (Kerlinger & Pedhazar, 1973). (*Note:* Table 3 shows ratios of between approximately 13 and 38 participants per predictor variable for the final equations developed in this study). An information sheet detailing all aspects of the study was given to participants prior to them providing written consent to participate. The research ethics boards for the participating university and hospital approved all methods and experimental procedures.

Instrumentation and Procedures

The data collection procedures followed in this study were identical to those reported previously for younger adults (Gyemi, et al., 2017). Flexible measuring tapes, anthropometers (Layfayette Instrument Company, Layfayette, IN) and skinfold callipers (Slimguide®, Creative Health Products, Plymouth, MI) were used to take 32 anthropometric measurements (Table 1: nine lengths, seven circumferences, eleven breadths and five skinfolds) were collected from participants while they stood in anatomical position by teams of two investigators trained on the proper techniques for collecting reliable anthropometric data. These measurements have been shown to have good between- and within-measurer reliability, with coefficients of variation (CVs) of <10% for all measurements (George et al., 2017). Participant age, sex, height and body mass were also recorded.

Once the anthropometric measurements were recorded, participants underwent a full-body DXA scan (GE Lunar Prodigy Advance: scan pixel resolution of 1.2 mm x 1.8 mm; mass resolution of 0.01 g/mm^2; scan time ~5 min) while supine. To determine the actual tissue masses specific to the head, neck, trunk, and pelvis, the DXA scans were analyzed using enCORE™ software (2013, GE Healthcare, v. 15.00.362) by creating custom regions of interest (ROIs) for each segment. The regional borders dividing the extremities from the core segments were made consistent with previously reported research (Holmes et al., 2005; Arthurs & Andrews, 2009; Burkhart et al., 2009; Gyemi et al., 2017), in which specific anatomical landmarks and techniques (Dempster, 1955; Clarys, Martin, & Drinkwater, 1984) were used to minimize tissue misattribution in the frontal plane between the lower extremities and pelvis, and upper extremities and trunk, respectively. Similarly, distinct anatomical landmarks were also utilized to help establish regional borders between the core segments (head and neck: the curvature of the inferior edge of the mandible; neck and trunk: the superior aspects of the clavicles; trunk and pelvis: the superior aspects of the iliac crests). Manual segmentation of the DXA scans to obtain tissue mass estimates (WM, FM, LM, BMC) for the head, neck, trunk, and pelvis was performed twice by the same analyst (~3 weeks apart). An internal study of the within-analyst reliability for these measures was determined to be excellent (CVs from 0.00% to 6.83%).

Analyses and Statistics

The data set was then inspected for missing or miss-keyed values and the presence of outliers, and normality was examined via histograms and Q-Q plots. Two sub-samples of participants were randomly created: a generation sample (n = 76: 38 M, 38 F), used to generate the tissue mass prediction equations, and a validation sample (n = 25: 13 M, 12 F), used to assess equation accuracy (Holmes et al., 2005; Arthurs & Andrews, 2009; Gyemi et al., 2017). Differences in tissue masses between the DXA segmentation trials, as well as the physical characteristics and anthropometric measures between sexes for the generation sample, were tested using independent samples t-tests. Independent samples t-tests and Levene's tests were also used to determine if the mean scores and variances between the generation and validation samples were homogenous. Ratios of the skewness and kurtosis statistics to their respective standard errors were calculated to examine normality of the generation sample; distributions were considered normal if ratios did not greatly exceed ± 1.96 at $P < 0.05$ (Stevens, 2002). To reduce multicollinearity, several highly correlated predictor variables ($r \geq 0.8$) were identified using correlation matrices and either combined into construct variables through Principal Component Analysis or removed from the regression analysis (Talmage et al., 1986), based on the reliability of their measurement (George et al., 2017). Overall, 16 prediction equations (four body segments: head, neck, trunk, pelvis x four tissue types: FM, LM, WM, BMC) were generated using multiple linear step-wise regression (SPSS 22 - IBM SPSS Statistics, IBM Corporation, Somers, NY), with personal (sex, age) and anthropometric data as predictors of tissue mass.

Table 1. Description of anthropometric measurements taken and recorded to the nearest millimetre from the head, neck, trunk, and pelvis

Measurements	Segment	Description and landmarks
Lengths	Pelvis (A)	Vertical distance between the pubic symphysis and the most superior point of the iliac crests
	Pelvis (L)	Vertical distance between the greater trochanter and the most superior point on the iliac crest
	Abdomen (A)	Vertical distance between the most superior point of the iliac crests and the xiphoid process of the sternum
	Thoracic (A)	Distance between the xiphoid process and the suprasternal notch of the sternum
	Trunk (L)	Distance between the most superior point of the iliac crests and the acromion
	Trunk (P)	Vertical distance between the posterior superior iliac spines and the top edge of the spinous process of C7
	Neck (A)	Distance between the suprasternal notch and the base of the mandible, with a closed mouth and neutral spine
	Neck (P)	Distance between the top edge of the spinous process of C7 and the base of the external occipital protuberance
	Head	Vertical distance between the base of the mandible and the top of the skull
Circumferences*	Hips	Horizontal distance around the hips at the level of the greater trochanters of the femurs
	Pelvis	Horizontal distance around the pelvis at the level of the superior aspects of the iliac crests
	Waist	Horizontal distance around the trunk at the level midway between the last ribs and the most superior point of the iliac crests
	Underbust	Horizontal distance around the trunk at the level of the xiphoid process
	Bust	Maximum distance around the trunk between the xiphoid process and the suprasternal notch of the sternum
	Neck	Distance around the neck, perpendicular to the long axis, at the level of C6
	Head	Horizontal distance around the head at the level supraorbital margins
Breadths*	Pelvis (M-L)	Distance across the hips at the level of the maximum circumference in the frontal plane
	Pelvis (A-P)	Distance across the pelvis at the level of the sacral hiatus along the antero-posterior axis.
	Waist (M-L)	Distance across the abdomen at the level of the waist circumference along the medio-lateral axis
	Waist (A-P)	Distance across the abdomen at the level of the waist circumference along the antero-posterior axis
	Chest (M-L)	Distance between the anterior axillary folds
	Chest (A-P)	Distance across the chest at the level of the xiphoid process along the antero-posterior axis
	Breast (A-P)	Distance across the thoracic region at the level of the bust circumference along the antero-posterior axis
	Sternum (A-P)	Distance across the thoracic region at the level of the suprasternal notch along the antero-posterior axis
	Shoulders (M-L)	Distance between the acromions
	Head (M-L)	Distance across the head at the level of the mandibular fossa along the medio-lateral axis
	Head (A-P)	Distance across the head at the level of the external occipital protuberance along the antero-posterior axis
Skinfolds**	Subscapular	Oblique fold (45 degree angle) 1 cm below the inferior angle of the scapula
	Mid-axillary	Vertical fold on the mid-axillary line at the level of the xiphoid process of the sternum
	Chest	Oblique fold one third of the way down the line between the anterior axillary fold and the nipple (closer to the axilla); for men, the distance is increased to halfway
	Suprailiac	Oblique fold taken in line with the natural angle of the iliac crest immediately superior to the iliac crest.
	Abdomen	Vertical fold 2 cm to the right side of the umbilicus

A = anterior; P = posterior; M = medial; L = lateral; A-P = antero-posterior; M-L = medio-lateral. *All circumferences and breadths/depths measured after a normal exhalation. Participants were also instructed to stand with feet slightly narrower than shoulder width, in a normal, relaxed state. **Skinfold locations parallel those from Jackson & Pollock (1978).

Data from the validation sample were then input into the prediction equations. The resulting predicted tissue masses were compared to the actual tissue masses for each ROI (as measured by DXA segmentation) using calculations of ab-

solute error, mean relative (%) error and root-mean-squared error. The strength of the relationships between the predicted and actual tissue masses for each ROI were determined using simple linear regression and depicted with scatterplots.

RESULTS

Tissue masses between the two DXA segmentation trials did not significantly differ ($P > 0.05$). Generation and validation samples showed no significant differences in terms of their mean scores and variances ($P > 0.05$); however, significant differences were noted in the generation sample between sexes for certain physical characteristics and anthropometric measures ($P < 0.05$) (Table 2). The total number of predictors was reduced from 36 variables to 20 (see Table 3 footnote) following correlation analyses, and two separate construct variables for head BMC (x_{19} = head length [0.930] + head breadth (A-P) [0.930]) and head LM ($x20$ = head length [0.850] + head circumference [0.897] + head breadth (M-L) [0.799]) were created.

Adjusted R^2 values for the tissue mass prediction equations (Table 3) ranged from 0.326 (head BMC) to 0.949 (trunk WM). In general, prediction equations for BMC had the lowest explained variance across all segments (adjusted $R^2 \leq 0.665$), while equations for WM demonstrated the highest explained variance for three of the four core segments (adjusted R^2 values ≥ 0.924 for the head, trunk, and pelvis). Standard errors ranged from 3.7 g to 1590.5 g for neck BMC and trunk FM, respectively (Table 3).

The largest mean errors between the actual and predicted tissue masses for all segments were found for the trunk (FM: 424.6 g LM: -380.0 g; WM: 283.8 g; BMC: -24.0 g) (Table 4). However, mean relative errors for all prediction equations were less than ± 3.0%, with the exception of trunk FM (6.1%). Root-mean-squared errors ranged from 3.3 g for neck BMC to 1857.0 g for trunk FM. Pearson correlations revealed that 15 of the 16 equations had significant moderate to strong relationships between the predicted tissue masses and the actual tissue masses measured by DXA ($P < 0.01$), with R^2 values ranging from 0.403 to 0.963 (Figure 1a-p). The sole exception was head BMC ($R^2 = 0.092$) ($P = 0.140$). Nonetheless, independent samples t-tests showed no significant differences between actual and predicted tissue mass values for any of the equations ($P < 0.05$).

DISCUSSION

The current study on older adults extends previous work that reported tissue mass prediction equations for the lower extremities (Holmes et al., 2005), upper extremities (Arthurs & Andrews, 2009) and core body segments (Gyemi et al., 2017) of younger adult populations using anthropometric measurements as predictors of segment tissue masses in vivo. Adjusted R^2 values for 11 of the 16 equations were found to be fairly high (≥ 0.715), with only two equations having moderate to weak values (neck BMC = 0.568; head BMC = 0.326). Overall, the prediction equations presented here demonstrated similar adjusted R^2 values and trends to those reported by Gyemi et al. (2017) for the same segments of younger adults. Specifically, BMC and FM equations for the head and neck had the lowest adjusted R^2 values (0.326 to 0.621) across all equations, with the exception of neck FM (0.768). Moreover, the tissue mass prediction equations in this study were found to explain less variance than those previously developed for the extremities (Holmes et al., 2005; Arthurs & Andrews, 2009), as was the case for the head, neck, trunk, and pelvis equations of younger adults (Gyemi et al., 2017). This may be due to the higher variability of tissue composition that makes up the core segments of the body (e.g., abdominal organs, lungs, brain, heart, etc.) compared to the more homogeneous composition of the extremities (Gyemi et al., 2017).

Minor tissue misattribution between the head and neck ROIs may have contributed to the lower explained variance for these core body segments in general, as well as the poorer correlations observed between predicted and actual tissue masses, particularly for head BMC ($R^2 = 0.092$) and FM ($R^2 = 0.403$) (Gyemi et al., 2017). Since all DXA scans were taken in the frontal plane, a small amount of neck tissue posterior to the jaw (e.g., the superior cervical vertebrae) was consistently characterized as head tissue when defining the border between the two segments. As per Gyemi et al (2017), although scanning the head and neck in the sagittal plane would have likely provided more accurate tissue mass values and better reflected the anthropometric measurements taken for these segments (e.g., anterior and posterior neck length), combining the head and neck tissue masses into one region for the regression analyses did not improve results. Therefore, the use of these equations in practice, especially for predicting segment BMC masses, should be done with consideration, until the accuracy and generalizability of the equations can be improved through enhanced scanning and analysis procedures, and increased sample sizes, respectively.

On average, the BMC prediction equations reported here for older adults resulted in lower adjusted R^2 values than previous equations developed for younger adults (Holmes et al., 2005; Arthurs & Andrews, 2009; Gyemi et al., 2017), especially when comparing the adjusted R^2 values for the head, neck, trunk, and pelvis BMC equations (0.326 – 0.665) to the equations for the upper (0.854 – 0.866) and lower (0.673 – 0.745) extremities. This may be due to the geometry and position of the bones within the core body segments, which tend to be more irregularly shaped and located deeper to the skin surface compared to the bones of the extremities, thus, limiting the ability of external anthropometric measurements to predict individual differences in bone tissue masses. Regarding the differences in the head, neck, trunk, and pelvis BMC equations between the two age populations, adjusted R^2 values for the older adults (0.553) were only marginally lower than those for the younger adults (0.562), on average. The younger adult BMC equations had higher adjusted R^2 values for the trunk (0.758) and pelvis (0.722) segments (Gyemi et al., 2017), while the older adult BMC equations had higher adjusted R^2 values for the head (0.326) and neck (0.568) segments. Considering that the age range of the older adult population

Table 2. Mean (± *SD*) physical characteristics and anthropometric measures for male and female participants from the generation and validation samples

Variable/Measure	Generation Sample (*n* = 76)				Validation Sample (*n* = 25)			
	Males (*n* = 38)		Females (*n* = 38)		Males (*n* = 13)		Females (*n* = 12)	
Physical characteristics								
Age (years)	49.4	(8.5)	49.3	(6.7)	49.4	(8.8)	48.2	(7.9)
Height (cm)	1.78*	(0.07)	1.62	(0.07)	1.78	(0.07)	1.64	(0.04)
Body Mass (kg)	85.8*	(17.0)	68.7	(12.6)	88.6	(12.2)	72.6	(17.9)
Lengths (cm)								
Pelvis (A)	14.9	(2.9)	15.8	(3.9)	15.3	(3.0)	16.5	(2.1)
Pelvis (L)**	12.7*	(1.8)	10.7	(2.8)	12.2	(2.1)	10.4	(2.6)
Abdomen (A)	22.9	(3.1)	21.5	(3.1)	22.2	(3.3)	24.0	(4.0)
Thoracic (A)**	18.9	(2.2)	18.7	(1.7)	19.0	(1.7)	17.9	(1.6)
Trunk (L)	43.0*	(3.1)	38.7	(2.5)	42.1	(3.1)	39.2	(2.2)
Trunk (P)	53.6*	(3.5)	48.2	(3.2)	53.6	(3.0)	50.6	(2.6)
Neck (A)	10.2*	(1.9)	8.5	(1.4)	9.9	(1.2)	8.9	(2.0)
Neck (P)	11.1*	(1.5)	9.5	(2.0)	10.4	(1.9)	9.6	(1.5)
Head	25.9*	(1.0)	24.4	(0.7)	26.3	(0.6)	24.8	(0.7)
Circumferences (cm)								
Hips	101.4	(8.1)	102.9	(9.3)	103.8	(6.2)	102.9	(14.0)
Pelvis	95.3	(11.7)	95.9	(10.8)	97.0	(11.1)	96.0	(18.6)
Waist	95.4*	(12.9)	87.9	(13.5)	98.4	(12.0)	87.8	(17.4)
Underbust	97.9*	(10.1)	84.8	(9.1)	100.3	(8.9)	85.9	(14.5)
Bust	102.9*	(10.2)	97.2	(10.5)	105.3	(9.5)	97.8	(14.6)
Neck	40.8*	(3.9)	33.9	(2.7)	40.1	(2.5)	34.8	(3.4)
Head	58.2*	(1.8)	55.6	(2.0)	58.4	(2.0)	55.9	(1.7)
Breadths (cm)								
Pelvis (M-L)	35.7	(2.3)	36.1	(3.3)	36.5	(2.4)	36.0	(3.9)
Pelvis (A-P)	19.8	(2.5)	19.8	(2.5)	20.0	(2.6)	19.1	(3.2)
Waist (M-L)	33.4*	(3.5)	30.4	(3.5)	34.4	(3.2)	30.4	(5.3)
Waist (A-P)	23.9	(4.6)	22.8	(4.2)	25.3	(4.3)	22.9	(6.0)
Chest (M-L)	35.4*	(3.0)	31.6	(2.7)	35.8	(2.2)	33.1	(3.3)
Chest (A-P)	23.5*	(3.3)	21.3	(3.7)	24.6	(3.5)	22.6	(4.6)
Breast (A-P)	25.7	(3.1)	25.7	(3.9)	26.8	(3.7)	26.1	(4.2)
Sternum (A-P)	17.8*	(2.1)	14.6	(1.7)	17.4	(1.4)	14.8	(2.1)
Shoulders (M-L)	41.0*	(2.2)	36.5	(2.6)	41.3	(3.0)	37.1	(2.7)
Head (M-L)	14.5*	(1.0)	13.5	(0.7)	14.8	(0.9)	13.6	(0.9)
Head (A-P)	20.0*	(0.7)	19.1	(0.7)	20.1	(0.6)	19.1	(0.8)
Skinfolds (mm)								
Subscapular	20	(10.0)	21	(8.4)	21	(8.4)	20	(11.0)
Midaxillary	16	(8.8)	16	(8.7)	16	(8.5)	18	(9.3)
Chest	11	(7.2)	13	(7.8)	12	(6.1)	17	(11.5)
Suprailiac	20	(10.4)	21	(8.0)	21	(7.8)	20	(9.7)
Abdomen	29	(11.6)	26	(9.7)	28	(10.7)	30	(13.9)

A = anterior; P = posterior; M = medial; L = lateral.*$P < 0.05$, significant difference between sexes within generation sample.**Average of lateral measurements from the left and right side of the body

examined in this study (36-65 years) is essentially twice as wide as the younger populations previously analyzed for the extremities (17-30 years) (Holmes et al., 2005; Arthurs & Andrews, 2009) and core segments (16-35 years) (Gyemi et al., 2017), these findings could be attributable to the increased variability in bone mineral density that occurs with

Table 3. Prediction equations, adjusted R^2 and standard errors (SEE) (g) for BMC, FM, LM and WM of the head, neck, trunk, and pelvis

Mass Type and Segment	Eq. #	Adj. R^2	SEE (g)
Bone Mineral Content (BMC)			
$Y(head) = -801.700 + 29.922x_{19} - 62.164x_2$	1	0.326	59.4
$Y(neck) = -11.210 + 2.848x_2 + 0.133x_4 + 1.151x_6 + 0.122x_1$	2	0.568	3.7
$Y(trunk) = -228.322 + 12.973x_5 + 2.855x_4 + 82.265x_2$	3	0.665	81.5
$Y(pelvis) = -370.605 + 325.174x_3 + 2.554x_4 - 2.879x_{16}$	4	0.653	49.5
Fat Mass (FM)			
$Y(head) = 518.175 + 8.913x_4 + 9.343x_{17} + 8.833x_{16}$	5	0.621	201.5
$Y(neck) = -316.541 + 3.277x_{15} + 5.242x_{10} + 2.597x_1 + 2.368x_{17}$	6	0.768	38.1
$Y(trunk) = -25098.395 + 199.730x_9 + 112.477x_{18} - 3544.304x_2 + 401.850x_{13}$	7	0.882	1590.5
$Y(pelvis) = -8228.340 + 96.843x_8 + 34.549x_{16} + 103.115x_{12} - 254.279x_2$	8	0.883	538.8
Lean Mass (LM)			
$Y(head) = -4399.313 + 447.690x_2 + 74.066x_{20} - 8.522x_{18}$	9	0.796	223.4
$Y(neck) = 2.044 + 132.673x_2 + 3.197x_4 - 5.708x_{16} + 2.527x_{18} + 11.341x_6$	10	0.774	67.2
$Y(trunk) = 4332.201 + 4276.003x_2 + 170.338x_4 - 67.893x_{18} - 66.96x_{16}$	11	0.890	1437.0
$Y(pelvis) = -3495.675 + 4039.597x_3 + 55.558x_4 - 47.088x_{18} + 731.606x_2$	12	0.788	692.0
Wobbling Mass (WM)			
$Y(head) = -4993.113 + 13.851x_4 + 84.248x_{11} + 128.424x_7 + 225.536x_2$	13	0.924	168.4
$Y(neck) = -656.216 + 32.233x_{10}$	14	0.715	97.1
$Y(trunk) = -19767.877 + 233.263x_4 + 126.163x_9 + 451.863x_{13}$	15	0.949	1580.5
$Y(pelvis) = -2752.395 + 110.619x_4 + 51.092x_8 - 21.821x_{18}$	16	0.925	628.4

Where: x_1 = age (yrs), x_2 = sex (f = 0, m = 1), x_3 = height (m), x_4 = body mass (kg), x_5 = trunk length (L) (cm), x_6 = neck length (A) (cm), x_7 = head length (cm), x_8 = pelvis circumference (cm), x_9 = waist circumference (cm), x_{10} = neck circumference (cm), x_{11} = head circumference (cm), x_{12} = pelvis breadth (A-P) (cm), x_{13} = chest breadth (M-L) (cm), x_{14} = chest breadth (A-P) (cm), x_{15} = subscapular skinfold (mm), x_{16} = chest skinfold (mm), x_{17} = suprailiac skinfold (mm), x_{18} = abdomen skinfold (mm), x_{19} = head length (cm) + head breadth (A-P) (cm), x_{20} = head length (cm) + head circumference (cm) + head breadth (M-L) (cm)

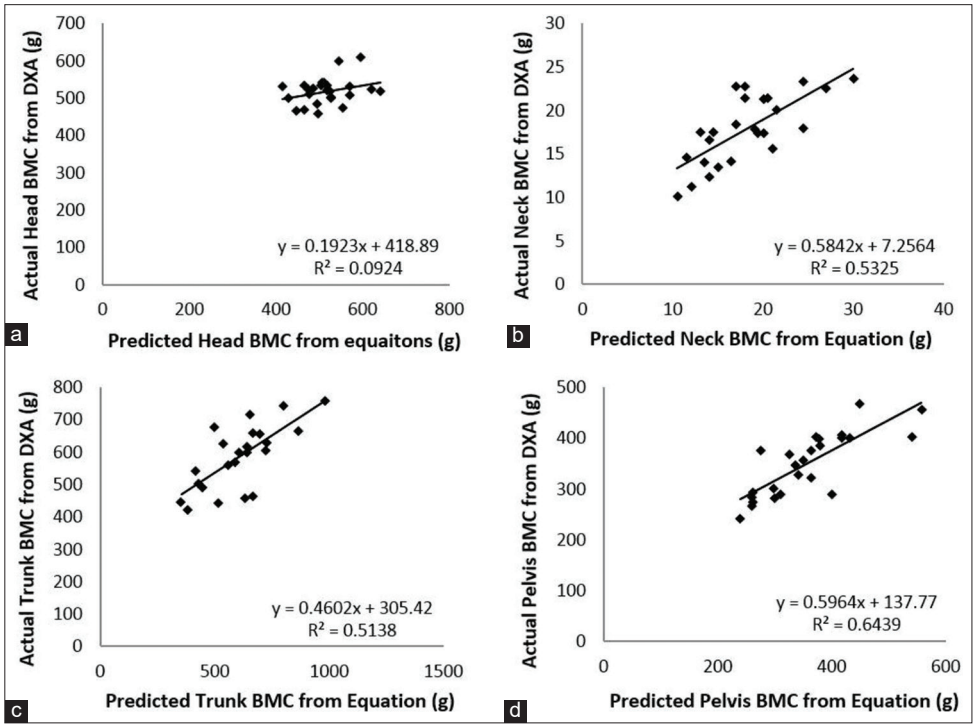

Figure 1. Relationships between predicted and actual tissue masses. Bone mineral content (BMC) for the head (a), neck (b), trunk (c), and pelvis (d). (*Continued*)

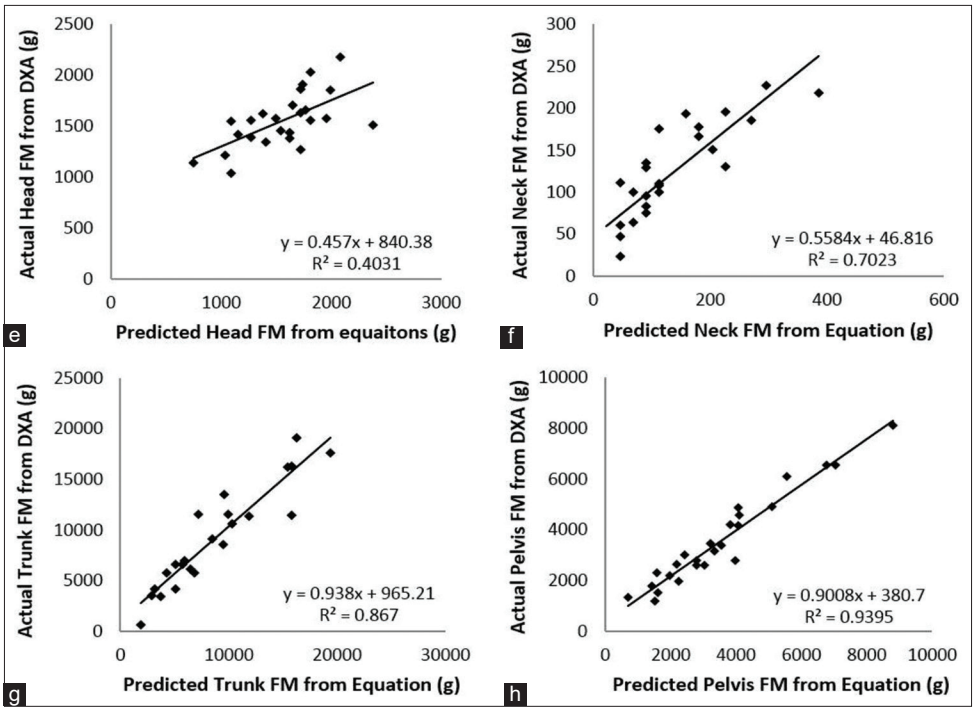

Figure 1. Relationships between predicted and actual tissue masses. Fat mass (FM) for the head (e), neck (f), trunk (g), and pelvis (h). (*Continued*)

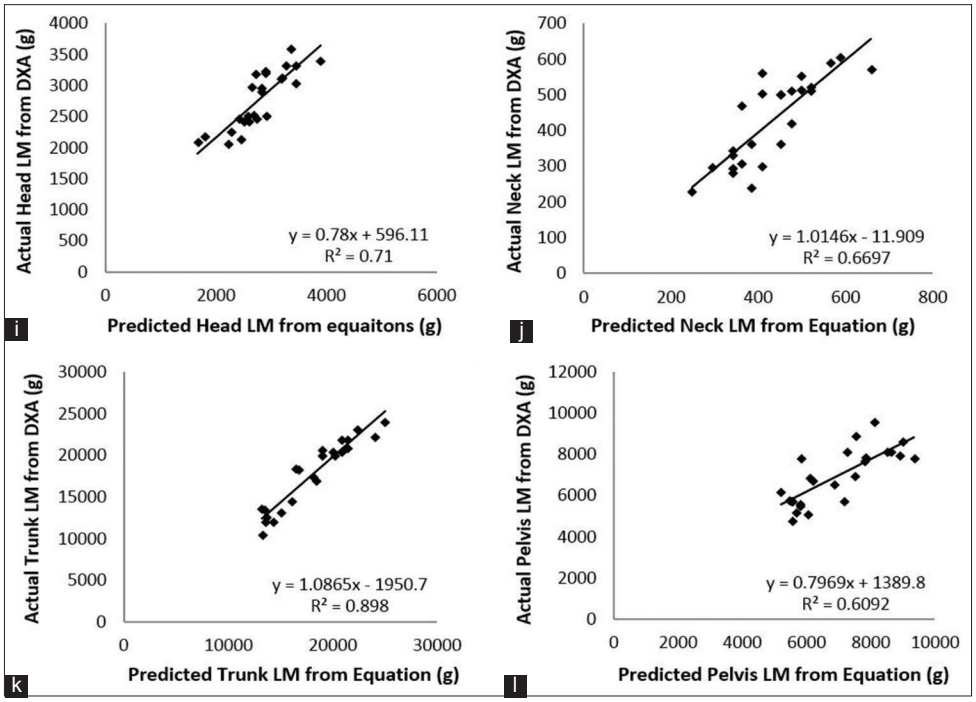

Figure 1. Relationships between predicted and actual tissue masses. Lean mass (LM) for the head (i), neck (j), trunk (k), and pelvis (l). (*Continued*)

age (Talmage et al., 1986; Wishart et al., 1995; Bernsten et al., 2001), which also cannot be accurately accounted for by external anthropometric measurements.

The tissue mass predication equations presented here complement previous work for younger adults (Holmes et al., 2005; Arthurs & Andrews, 2009; Gyemi et al., 2017) by enabling the estimation of segment tissue masses that account for changes in body composition that naturally occur with age (Baumgartner, 2000). The results of the current study also bring the literature closer to having a full set of equations for the entire body across a broad age range in both males and females. Future research should develop and validate similar equations for the upper and lower extremities of older adults, as they have not been completed to date. A full set of population-specific tissue mass estimates from living people would help improve biomechanical mod-

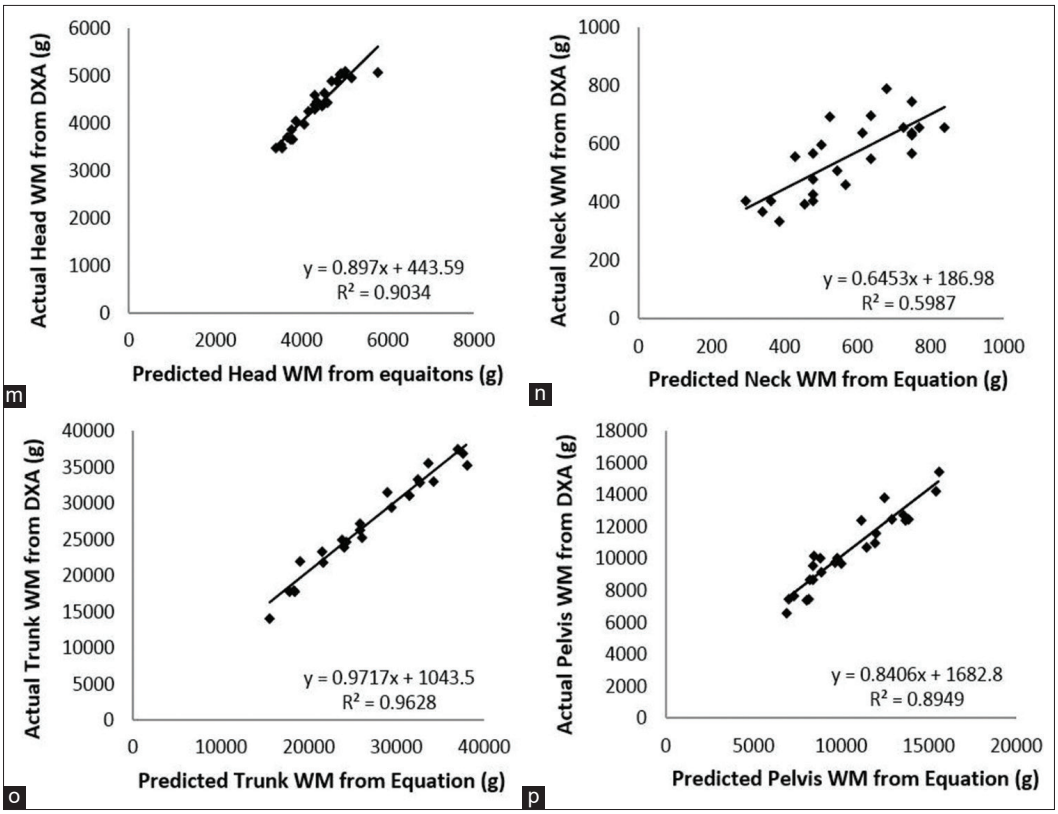

Figure 1. Relationships between predicted and actual tissue masses. Wobbling mass (WM) for the head (m), neck (n), trunk (o), and pelvis (p)

Table 4. Mean (± *SD*) predicted and actual (DXA) masses and errors from the validation sample (n = 25 for head, neck, and pelvis; n = 23 for trunk)

Tissue and Segment	Predicted (g)		Actual (g)		Error (g)		% Error		RMS_{error} (g)
BMC									
Head	518.1	(35.0)	515.9	(55.4)	2.2	(55.8)	1.3	(10.8)	54.7
Neck	17.8	(4.0)	18.1	(4.9)	-0.3	(3.4)	1.1	(18.3)	3.3
Trunk	586.3	(99.4)	610.3	(154.8)	-24.0	(108.6)	-0.7	(18.2)	108.9
Pelvis	349.7	(61.8)	355.4	(83.2)	-5.7	(49.9)	0.2	(12.9)	49.2
FM									
Head	1556.0	(269.4)	1565.8	(374.2)	-9.8	(290.9)	2.8	(19.8)	285.2
Neck	122.3	(60.7)	135.2	(91.1)	-12.9	(52.1)	-0.3	(47.8)	52.6
Trunk	9144.4	(4997.6)	8719.8	(4960.9)	424.6	(1848.5)	6.1	(25.9)	1857.0
Pelvis	3512.0	(1947.4)	3544.4	(1809.8)	-32.4	(485.2)	-1.7	(18.5)	476.5
LM									
Head	2768.4	(470.6)	2785.1	(508.4)	-16.6	(277.0)	0.2	(10.8)	271.9
Neck	426.2	(120.3)	431.8	(97.0)	-5.6	(69.1)	-1.6	(16.9)	68.0
Trunk	17783.4	(4160.5)	18163.4	(3628.8)	-380.0	(1365.2)	-2.6	(8.6)	1388.2
Pelvis	6918.6	(1344.2)	6938.1	(1316.6)	-19.5	(881.8)	0.3	(12.9)	864.2
WM									
Head	4347.1	(565.1)	4351.8	(598.8)	-4.6	(186.1)	0.0	(3.7)	182.4
Neck	553.4	(128.3)	567.9	(153.9)	-14.5	(97.9)	-0.1	(17.8)	97.0
Trunk	27170.0	(6801.4)	26886.2	(6867.8)	283.8	(1325.5)	1.2	(5.4)	1327.0
Pelvis	10497.4	(2358.5)	10486.1	(2654.3)	11.2	(873.7)	1.0	(8.5)	856.2

RMS_{error} = root-mean-squared error, BMC = bone mineral content, FM = fat mass, LM = lean mass, WM = wobbling mass. Validation sample for trunk equations excluded two participants (n = 23: 13 M, 10 F) due to the additional mass associated with breast implants

elling efforts using body segments whose tissue composition is known to vary as a function of age (Baumgartner, 2000) and sex (Gallagher et al., 1996), as body composition changes such as these will have an influence on analyses of impact-related events (Pain & Challis, 2006; Schmitt & Günther, 2010; Bazrgari et al., 2011), that are consistent with sport and recreational activities. In addition, future research should determine whether it would be feasible to also scan participants in the sagittal plane to provide a better view of the neck region. This would help to facilitate the segmentation of the neck from the DXA scans, which would reduce the possible tissue misattribution between the neck and the head segments, thereby improving tissue mass predictions for the neck and head. Given the age ranges previously studied and the changes is body composition that occur with age, establishing tissue mass prediction equations for an even older group of adults (> 65 years of age), that also consider other factors (e.g., physiological measures affecting tissue composition) as predictor variables, would be a positive contribution to the literature.

CONCLUSIONS

In conclusion, regression equations were generated and validated for an older adult population (older than previously studied participants who were mostly university-aged) that allow soft and rigid tissue masses of the head, neck, trunk, and pelvis to be accurately predicted in vivo using anthropometric measurements and personal variables, including age and sex. The practicality of these equations makes them useful tools for acquiring tissue mass estimates of core body segments of living older adults, however, further research is needed to help improve the predictive capacity of the BMC equations. Ultimately, this work will facilitate the development of person-specific biomechanical models that incorporate both rigid and non-rigid tissue elements, which will enhance our understanding of highly dynamic impact events associated with human movement.

ACKNOWLEDGEMENTS

Thank you to NSERC for funding, and to Diagnostic Imaging at the Metropolitan Campus of Windsor Regional Hospital for the use of their facility. Also, thanks to Alex Waugh, Kristine Silva, Jordyn Severin, Caroline Nelson and Ben Warnock for their assistance with data collection.

REFERENCES

Arthurs, K. L., & Andrews, D. M. (2009). Upper extremity soft and rigid tissue mass prediction using segment anthropometric measures and DXA. *Journal of Biomechanics,* 42(3), 389-394. DOI: 10.1016/j.jbiomech.2008.11.021

Baumgartner, R. N. (2000). Body composition in healthy aging. *Annals of the New York Academy of Sciences,* 904, 437-438. DOI: 10.1111/j.1749-6632.2000.tb06498.x

Bazrgari, B., Nussbaum, M. A., Madigan, M. L., & Shirazi-Adl, A. (2011). Soft tissue wobbling affects trunk dynamic response in sudden perturbations. *Journal of Biomechanics,* 44(3), 547-551. https://doi.org/10.1016/j.jbiomech.2010.09.021

Bernsten, G. K. R., Fønnebø, V., Tollan, A., Søgaard, A. J., & Magnus, J. H. (2001). Forearm bone mineral density by age in 7,620 men and women. *American Journal of Epidemiology,* 153(5), 465-473. https://doi.org/10.1093/aje/153.5.465

Burkhart, T. A., Arthurs, K. L., & Andrews, D. M. (2009). Manual segmentation of DXA scan images results in reliable upper and lower extremity soft and rigid tissue mass estimates. *Journal of Biomechanics,* 42(8), 1138-1142. https://doi.org/10.1016/j.jbiomech.2009.02.017

Clarys, J. P., Martin, A. D., & Drinkwater, D.T. (1984). Gross tissue weights in the human body by cadaver dissection. *Human Biology,* 56(3), 459-473. https://www.jstor.org/stable/41463592

Dempster, W. T. (1955). *Space requirements of the seated operator*. Ohio, IL: Wright-Patterson Air Force Base (WADC TR 55-159). https://doi.org/10.1002/ajpa.1330220412

Gallagher, D., Visser, M., Sepúlveda, D., Pierson, R. N., Harris, T., & Heymsfield, S.B. (1996). How useful is body mass index for comparison of body fatness across age, sex, and ethnic groups? *American Journal of Epidemiology,* 143(3), 228-239. https://doi.org/10.1093/oxfordjournals.aje.a008733

George, N. C., Kahelin, C., Burkhart, T. A., & Andrews, D. M. (2017). Reliability of head, neck and trunk anthropometric measurements used for predicting segment tissue masses in living humans. *Journal of Applied Biomechanics,* 33(5), 373-378. https://doi.org/10.1123/jab.2016-0122

Gruber, K., Ruder, H., Denoth, J., & Schneider, K. (1998). A comparative study of impact dynamics: wobbling mass model versus rigid body models. *Journal of Biomechanics,* 31(5), 439-444. https://doi.org/10.1016/S0021-9290(98)00033-5

Gyemi, D. L., Kahelin, C., George, N. C., & Andrews, D. M. (2017). Head, neck, trunk and pelvis tissue mass predictions for young adults using anthropometric measures and DXA. *Journal of Applied Biomechanics,* 33(5), 366-372. https://doi.org/10.1123/jab.2016-0228

Holmes, J. D., Andrews, D. M., Durkin, J. L., & Dowling, J. J. (2005). Predicting in vivo soft tissue masses of the lower extremity using segment anthropometric measures and DXA. *Journal of Applied Biomechanics,* 21(4), 371-382. https://doi.org/10.1123/jab.21.4.371

Jackson A. S., & Pollock, M. L. (1978). Generalized equations for predicting body density of men. *British Journal of Nutrition,* 40(03), 497–504. https://doi.org/10.1079/BJN19780152

Kerlinger, F. N., & Pedhazar, E. S. (1973). *Multiple regression in behavioral research*. New York: Holt, Reinhart, & Winston.

Pain, M. T., & Challis, J. H. (2006). The influence of soft tissue movement on ground reaction forces, joint torques and joint reaction forces in drop landings. *Journal of*

Biomechanics, 39(1), 119-124. https://doi.org/10.1016/j.jbiomech.2004.10.036

Schmitt, S., & Günther, M. (2010). Human leg impact: energy dissipation of wobbling masses. *Archives of Applied Mechanics,* 81(7), 887-897. https://doi.org/10.1007/s00419-010-0458-z

Stevens, J. P. (2002). *Applied Multivariate Statistics for the Social Sciences*. 4th ed. Hillsdale, NJ: Lawrence Erlbaum Associates.

Tabachnick, B. G., & Fidell, L. S. (2013). *Using multivariate statistics*. 6th ed. Boston, MA: Pearson Education.

Talmage R. V., Stinnett, S. S., Landwehr, J. T., Vincent L. M., & McCartney, W. H. (1986). Age-related loss of bone mineral density in non-athletic and athletic women. *Bone and Mineral,*1(2), 115-125.

Wishart, J. M., Need, A. O., Horowitz, M., & Nordin, B. E. C. (1995). Effect of age on bone density and bone turnover in men. *Clinical Endocrinology,* 42(2), 141-146. https://doi.org/10.1111/j.1365-2265.1995.tb01854.x